ASSESSMENT OF WALLS' THERMAL RESPONSE FROM A PROPORTIONAL AND A RELATIVE POINT OF VIEW

Karolos J. Kontoleon[1], Dimitrios K. Bikas[2], Dimitrios G. Aravantinos[3], Aikaterini G. Tsikaloudaki[4], Theodoros G. Theodosiou[5]

[1-5] Laboratory of Building Construction & Building Physics (*LBCP*), Department of Civil Engineering, Faculty of Engineering, Aristotle University of Thessaloniki (*A.U.Th.*), Gr-541 24 Thessaloniki, Greece
e-mails: karolos_kontoleon@yahoo.com [1], bikasd@civil.auth.gr [2], demetre@civil.auth.gr [3], tgt@civil.auth.gr [4], katgt@civil.auth.gr [5];
web page: http://lbcp.civil.auth.gr/

Keywords: *heat transfer, transient analysis, dynamic thermal characteristics, proportional and relative metrics*

ABSTRACT

In this work the variations of masonry thermophysical properties for various wall configurations are considered to assess their influence on the fundamental thermal inertia parameters, such as the decrement factor f and the time lag φ. The investigated assemblies correspond to insulated brick walls with a fixed thickness and with the brick layer placed as one or two segments. Also, the insulation is placed as one layer on: (i) the external cross-section, (ii) the internal cross-section and (iii) the mid-centre of masonry, giving rise to a total of three wall assemblies. The thermal analysis is accomplished via a thermal-network model and by adopting the nodal solution method. Variations on the thermophysical properties of solid bricks are seen to interrelate non-linearly with the walls' RC-sections parameters with consequences on its dynamic thermal characteristics. Likewise, the location of insulation modifies critically the thermal behaviour of the studied wall configurations. These issues are approached by appropriate metrics for assessing thermal response from a proportional (PDM, PTM) and a relative (RDM, RTM) point of view. Computer results, revealing the influence of the assumed wall attributes on the decrement factor, time lag and the proposed metrics are shown in this paper.

1 INTRODUCTION

Building shells delineate the boundary between the interior and ambient environment. Designing adequately building envelopes is generally an integral task, which affects significantly the indoor thermal conditions. Among its most important benefits is the scale down of energy demands and the development of a superior temperature field for the users of buildings. The type of materials employed in building structures can widely affect the above, since their properties are associated with the heat transfer mechanisms. The geometrical characteristics and thermophysical properties of materials are responsible for the thermal resistances and capacitances in the heat flow paths of the building setup. In addition, the spatial position and allocation of building materials influence their thermal behaviour.

The attributes of the building's layer materials are capable to ameliorate the indoor environment. In terms of energy efficiency, the exploitation of high mass and high resistant materials is exceedingly valuable. As a result of their high heat capacity, masonry materials demonstrate the ability to store energy within their thermal mass (heat sink), while they can also shift the instant at which the peak temperatures appear at the interior surface of a wall. Nevertheless, it is important to mention that masonry materials show a low thermal resistance (high thermal conductivity). On the other hand, due to their low heat transmittance, insulation materials are suitable to diminish the heat transfer proliferation instead of thickening absurdly the masonry layer. Insulation materials respond like heat barriers that cause an evidential shrink of the temperature oscillation in the direction of heat flow. In contrast with masonry materials, insulation materials show a low thermal capacitance (low volumetric heat capacity). As it is clear, the combination of both masonry and insulation materials is decisive in order to generate a steadier indoor environment.

Until today, several studies have dealt with the measurement of the dynamic heat-transfer characteristics of building elements. In [1, 2] Asan has estimated the effect of wall's insulation thickness and position on decrement factor and time lag. In his study he determined the optimum insulation position for minimum decrement factor and maximum time lag. In a subsequent work, Ozel and Pihtili [3], have determined the optimum location and distribution of insulation for various types of wall configurations. In another study Al-Sanea and Zedan [4] have analysed numerically the dynamic thermal characteristics of insulated building walls with the same thermal mass and optimised insulation thickness, under steady periodic conditions. More recently Al-Sanea et al. [5, 6] have examined numerically the effects of a varying amount and location of thermal mass on the dynamic thermal characteristics; in addition, the effect of the type of masonry material and surface absorptivity on critical thermal mass thicknesses, for insulated building walls with a fixed nominal resistance under steady periodic conditions was studied. Moreover, in [7, 8] the influence of wall orientation and the exterior surface solar absorptivity on thermal inertia parameters have also been investigated. These studies considered periodic temperature oscillations of the outdoor environment corresponding to the Mediterranean region by taking into account the variable effect of solar radiation and orientation. On the above basis, Jin et al. in [9] proposed two new dynamic thermal parameters that correspond to the heat flux decrement factor and heat flux time lag that are valuable for reducing the energy demands and upgrade the indoor thermal conditions.

In the present work the effect of the brick density and thermal conductivity variations on decrement factor f and time lag φ of conventional insulated wall assemblies is analysed. An increase in the walls' masonry density lowers its thermal resistance but increases its potential for thermal storage that delays and reduces the heat propagation through the wall. On the other hand, a decrease in the walls' masonry density leads to opposite outcomes. According to these dependencies, the increase/decrease of the coefficient of thermal conductivity and density of masonry, decreases/increases the thermal resistance and increases/decreases the thermal capacity of the entire wall. In overall, the variation of the masonry density and conductivity, its placement and the allocation of insulation have an important bearing on the walls' thermal behaviour. As such variations, affect the decrement factor and time lag in a different fashion, metrics for assessing the walls' thermal behaviour from a proportional and a relative point of view are introduced. The heat transfer analysis is carried out by employing a thermal network model that simulates the transient behaviour of multilayer wall assemblies under the influence of a sinusoidal heat wave. The heat flow path takes into account: (a) conduction through the wall construction, (b) combined convection and radiation at the external and internal surface boundaries and (c) the forcing functions at both limits of the wall. In the following sections the above issues are presented comprehensively.

2 HEAT TRANSFER AND TRANSIENT PROBLEM

The one dimensional heat flow rate through a wall of thickness L with n layers (each layer with given geometrical characteristics and thermophysical properties) is subject to *Fourier's law*. The problem geometry for an n-layer wall assembly is shown in Fig. 1. The heat conduction governing equation at each point of a homogeneous wall layer in the time domain, is well defined [1, 2, 10, 11]:

$$k \cdot \frac{\partial^2 T}{\partial x^2} = \rho \cdot C_p \cdot \frac{\partial T}{\partial t} \tag{1}$$

where λ is the thermal conductivity, ρ is the density and C_p is the specific heat of the material layer. The above equation is applicable when: (a) the transverse heat flows are negligible, (b) heat is not generated within the thermal mass and (c) the thermophysical properties of materials are independent with temperature variations.

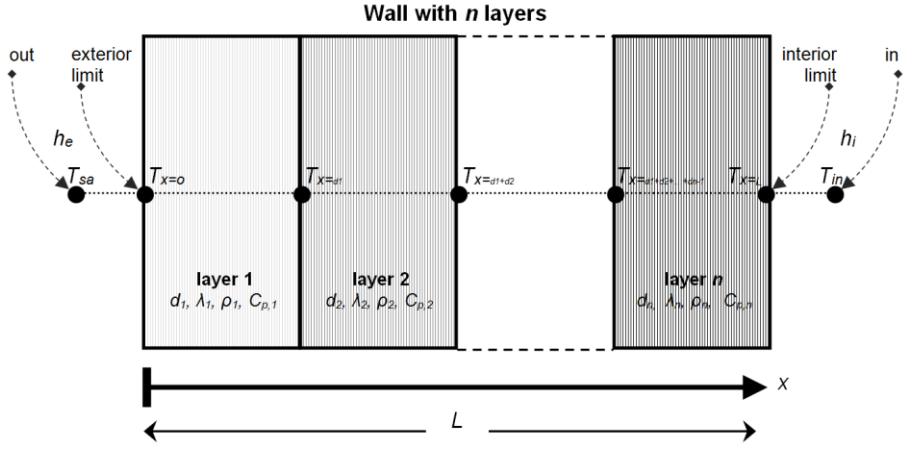

Figure 1. Outline of transient problem used for a multi-layered wall assembly.

Aiming to overcome Eq. (1), an initial condition and two boundary conditions are required.

- As an initial condition, the steady-state solution of the problem at $t = 0$ is considered.
- Regarding the exterior surface of the opaque wall the boundary condition due to convection is defined by *Newton's law*:

$$-\lambda \cdot \frac{\partial T(0,t)}{\partial x} = h_e \cdot (T_{sa} - T_e) \tag{2}$$

where h_e is the heat transfer coefficient due to combined convection and radiation, T_{sa} is sol-air temperature and T_e is the temperature at the exterior surface of the wall ($x = 0$). Evidently, the overall effect of long wave radiant heat exchange with the outdoors surroundings and incident solar radiation (direct, diffuse and reflective) is controlled by the fictitious sol-air temperature concept [1-3, 12]. In this study the T_{sa} is suitably assumed to show a sinusoidal periodic variation. It can be shown that for a sinusoidal excitation function of fixed amplitude and frequency the steady response will also be sinusoidal with the same frequency, but with a different fixed amplitude and a phase shift from the excitation function.

- At the interior surface of the opaque wall the boundary condition due to convection is defined by *Newton's law*:

$$-\lambda \cdot \frac{\partial T(L,t)}{\partial x} = h_i \cdot (T_i - T_{in}) \tag{3}$$

where h_i is the heat transfer coefficient due to combined convection and radiation, T_{in} is the indoor temperature and T_i is the temperature at the interior surface of the wall ($x = L$). The indoor temperature field, which incorporates the long wave radiant heat exchange with the indoor space, is presumed to be constant in the time domain.

As it is clear, Eqs. (2) - (3) balance the conduction heat transfer through the wall with the convective heat transfer between the exterior/interior wall surfaces, exposed to the outdoor/indoor environment, including the irradiative heat transfer.

3 MODELLING & ANALYSIS OF TRANSIENT PROBLEM

3.1 Thermal modelling

The present work employs the thermal network approach that allows the modelling of relatively composite heating problems by equivalence with the laws of electric circuits. Accordingly, node voltages and branch currents correspond to temperatures and heat flows, respectively. Likewise, electrical resistances and electrical capacitances correspond to thermal resistances and thermal capacitances [13, 14]. The matrix formulation that combines the topological and algebraic data of the thermal model allows the formation of a system of equations that can be resolved by one of the existing methods.

In Fig. 2 the employed *n*-layer lumped thermal-network model is delineated. As shown, for each material-layer, the model comprises a number ($j = 1$ to n) of discrete *RC*-sections with an inner and an outer thermal resistance and the thermal capacitance of the layer. Each capacitance models the ability of the material-layer to store energy within its thermal mass. For wall assemblies comprising a number of material-layers, the ability to store energy depends on the characteristics of the individual layer. The *RC*-section material temperature is at the common node of the resistive and capacitive elements. The resistances and capacitances of each *RC*-section are defined by:

$$R_j = \frac{d_j / 2}{\lambda_j \cdot A} \quad \text{[K/W]} \tag{4}$$

$$C_j = \rho_j \cdot C_{p,j} \cdot d_j \cdot A \quad \text{[J/K]} \tag{5}$$

with A and d_j corresponding to the j-section material area and thickness, respectively; λ_j is the thermal conductivity, ρ_j is the density and $C_{p,j}$ the specific heat of the j-section material.

The boundary conditions due to combined convection and radiation are modelled by two surface resistances between the exterior/interior surfaces of the wall and the outdoor/indoor environment limitations, respectively:

$$R_e = \frac{1}{h_e \cdot A} \tag{6}$$

$$R_i = \frac{1}{h_i \cdot A} \tag{7}$$

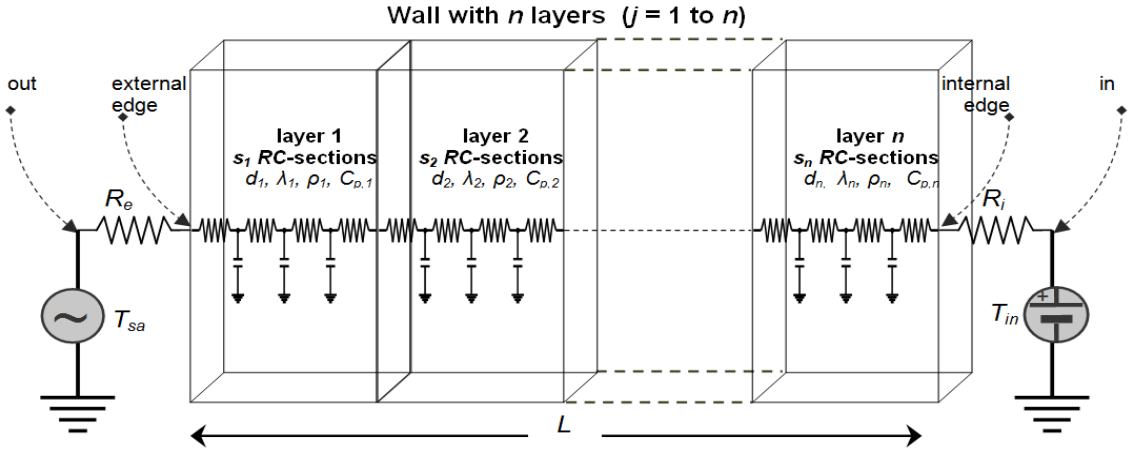

Figure 2. Thermal-network model of a multi-layered wall assembly.

The above resistances couple the exterior and interior boundary conditions on both wall surfaces with the outdoor forcing function T_{sa} and the fixed indoor source T_{in} described in section 2.

3.2 Thermal analysis

Another essential aspect that must be taken into consideration is the solution methodology of the heat transfer problem that has been formulated with the thermal circuit approach [7, 8, 13, 14]. As mentioned, the present study relies on the formulation of the nodal equations in matrix form; this is accomplished by appropriately modelling the thermal capacitances with thermal resistances in series with time-varying (updated at each solution-step) voltage sources. The stored energy within the various *RC*-sections of a wall is represented by the accumulated charge of the capacitors. In this study a typical time increment Δt = 60s is considered. The above methodology has been confirmed in previous studies, as it has shown to generate results virtually identical with those extracted by precise analytical solutions, under dynamic conditions. For the purpose of eliminating the initial effect of the transient heat process, the analysis is carried out for a period of *n*-days (a 10-day period is adequate to fully attain a steady periodic-state).

4 WALL CONFIGURATIONS

As a general rule, perforated brick walls show a moderate energy-saving advantage since they cannot store a considerable amount of heat due to their low thermal mass. Nevertheless, their use is dominant compared with traditional solid brick units. Despite the fact that perforated bricks are used very widely throughout Europe and the United States, little extensive work on the performance characteristics of solid brick walls has been published. The present investigation is on insulated solid brick walls with high thermal mass. Encapsulated thermal mass is critical for improving the indoor conditions under large daily temperature fluctuations.

The studied multi-layered wall arrangements consist of:

(a) Masonry *M* – solid brick (with thickness d_M = 20 cm as one layer, or d_M = 10 cm as two layers),

(b) Insulation *I* – extruded polystyrene *XPS* (with thickness d_I = 5 cm to be placed as one layer on the external cross-section, the internal cross-section or the mid-centre of masonry),

(c) Coating *C* – plaster on both the exterior and interior surfaces (with thickness d_C = 2 cm).

Accordingly, the cross sectional configurations, shown in Fig. 3, are denoted as *IM*, *MIM* and *MI*; the total thickness of all studied wall assemblies is 29 cm, while they show the same thermal resistance and capacitance.

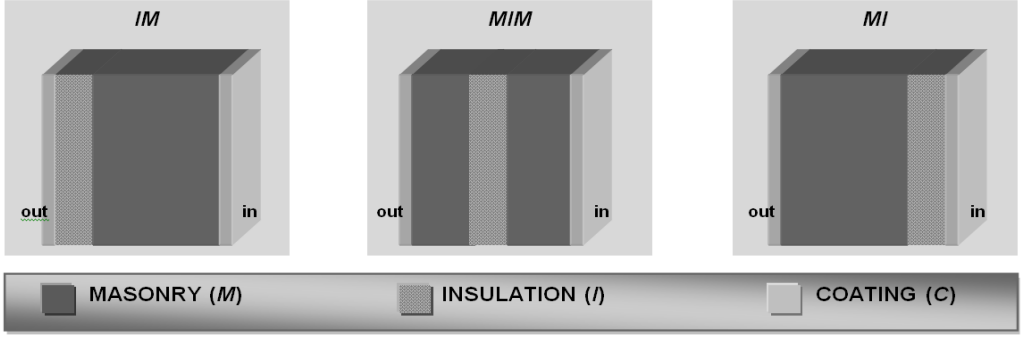

Figure 3. Analysed multi-layered wall configurations (insulated solid brick walls).

The present study further examines the influence of the masonry density and conductivity on the decrement factor and time lag. In general, several categories of solid bricks are produced with densities depending on the analogies of their ingredients. The graph of Fig. 4 shows the variation of conductivity λ_M with the density ρ_M for various types of solid bricks (low, medium or high density) [15]. The range of masonry's density values considered in this graph is large enough to cover most commonly used solid brick elements, varying from lightweight to heavyweight categories; these variations affect the thermal inertia parameters in a different fashion. This influence of masonry density and conductivity variations together with the various placements of materials is further discussed in the following section.

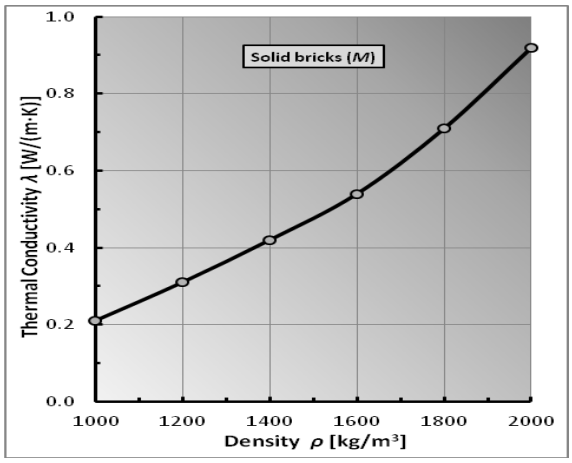

Figure 4. Non-linear dependence of thermal conductivity on masonry density.

5 RESULTS & DISCUSSION

5.1 Dynamic thermal characteristics

A fundamental issue of an efficient building design is the determination of the thermal behaviour of the elements that outline the building shell. The thermal performance of an opaque element depends on how well its materials restrain the heat, how fast the heat propagates through it and, finally, the outdoor/indoor forcing conditions and constraints at both its boundaries. The above aspects are adequately assessed by the decrement factor *f* and the time lag φ. The decrement factor refers to the ability of a wall element to attenuate the amplitude of the exterior surface temperature to that of the interior surface temperature; moreover, the time lag depicts the time delay of a heat wave to propagate from one side of a wall element to the other. The above parameters are defined by the following equations [1-9]:

$$f = \frac{T_{i,\max} - T_{i,\min}}{T_{e,\max} - T_{e,\min}} \tag{8}$$

$$\phi = t_{Ti,\max} - t_{Te,\max} \tag{9}$$

where *Ti,max*, *Ti,min*, *Te,max*, and *Te,min* correspond to the maximum and minimum temperatures on both the interior and the exterior surfaces of the assembly. Moreover, $t_{Ti,max}$ and $t_{Te,max}$ indicate the time points when the inside and the outside surface temperatures are at their peaks, respectively.

The graphs of Fig. 5(a) and (b) refer to the dependence of the decrement factor and time lag on the masonry's density and type of wall assembly.

As shown in Fig. 5(a), for the wall assembly *IM*, an increase of the density of masonry leads to an unwanted increase of the values of decrement factor *f*. Thus, for density ρ_M = 1000 kg/m^3 the optimal value (minimum) of the decrement factor is f_{IM} = 0.01076, while for ρ_M = 2000 kg/m^3 the worst value (maximum) is f_{IM} = 0.01668. Analogously, for the *MIM* and *MI* configurations the increase of masonry density results to the parallel raise of decrement factor values *f*. The corresponding *f* values for ρ_M = 1000 kg/m^3 are f_{MIM} = 0.01808 and f_{MI} = 0.01190; as for ρ_M = 2000 kg/m^3 the *f* values are f_{MIM} = 0.02516 and f_{MI} = 0.02172. From the above graphs, it is also obvious that the *MI* wall formation shows a greater sensitivity (with reference to the variations of masonry density) in comparison to the two other formations.

Comparing the above three discussed configurations, the optimal decrement factor is obtained when the insulation is placed at the external cross-sectional area of masonry (i.e., the *IM* assembly). Conversely, the worst

decrement factor is attained when the insulation is placed at the mid-centre of masonry (i.e., the *MIM* assembly). Coming to a classification of the decrement factor for these wall assemblies it can be easily seen that for the entire bandwidth of masonry densities it is $f_{IM} < f_{MI} < f_{MIM}$.

From Fig. 5(b), it can be seen that for the three wall assemblies there is a decrease in the values of time lag φ as the masonry density increases. Thus, the maximum and minimum values of φ is attained for ρ_M = 1000 kg/m^3 and ρ_M = 2000 kg/m^3, respectively. For a masonry densities ρ_M = 1000 kg/m^3 and ρ_M = 2000 kg/m^3 the time lag values for each one of the assumed configurations are: (a) φ_{IM} = 9.27 h and φ_{IM} = 7.43 h, (b) φ_{MIM} = 9.14 h and φ_{MIM} = 8.15 h and (c) φ_{MI} = 8.94 h and φ_{MI} = 6.97 h, respectively. In this figure it is also noticed that the *MIM* wall formation presents the lowest sensitivity alongside the variations of masonry density, compared to the other two formations (slow declination).

As for the time lag outcomes, its classification for the investigated wall assemblies for the masonry density range 1000 kg/m^3 $\leq \rho_M <$ 1200 kg/m^3 it is $\varphi_{IM} > \varphi_{MIM} > \varphi_{MI}$ and for1200 kg/m^3 $\leq \rho_M \leq$ 2000 kg/m^3 it is $\varphi_{MIM} > \varphi_{IM} > \varphi_{MI}$. Evidently, the worst time lag is constantly resulted when the insulation is placed at the internal cross-sectional area of masonry (i.e., the *MI* assembly). On the other hand, the wall configuration that succeeds optimal time lag shows dependence by the density of masonry.

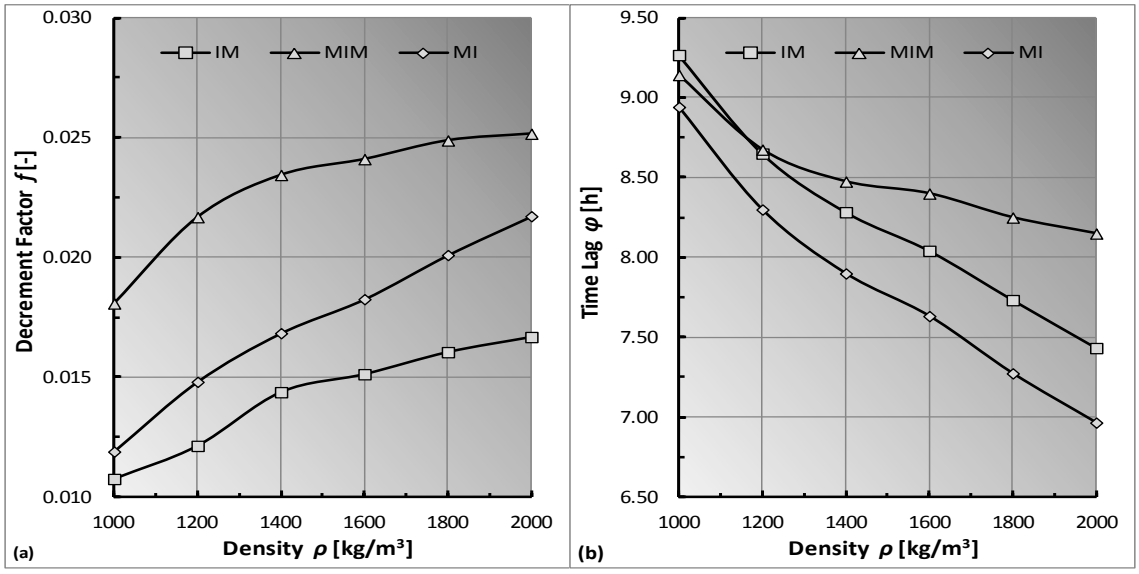

Figure 5. Decrement factor (a) and time lag (b) variation with masonry density and wall assembly.

5.2 Dynamic thermal response metrics

Following the results presented in the previous section, it becomes obvious that the variation of masonry density has a different impact on the decrement factor and time lag for each wall formation. Below two metrics with relevant results are proposed for assessing the merits of each wall formation from a proportional and a relative point of view. These metrics depict the potential for improving the thermal inertia parameters of a particular wall configuration [8].

- The proposed proportional metrics for the decrement factor, PDM_W (Proportional Decrement factor Metric), and for the time lag, PTM_W (Proportional Time lag Metric), are defined as:

$$PDM_W = \frac{f_{W,\max} - f_{W,r}}{f_{W,\max} - f_{W,\min}} x\,100\% \tag{10}$$

$$PTM_W = \frac{\phi_{W,r} - \phi_{W,\min}}{\phi_{W,\max} - \phi_{W,\min}} x\,100\% \tag{11}$$

- The proposed relative metrics for the decrement factor, RDM_W (Relative Decrement factor Metric), and for the time lag, RTM_W (Relative Time lag Metric), are defined as:

$$RDM_W = \frac{f_{W,\max}}{f_{W,r}} \tag{12}$$

$$RTM_W = \frac{\phi_{W,r}}{\phi_{W,\min}} \tag{13}$$

The subscript *W* denotes a particular wall formation (i.e., *IM*, *MIM* and *MI*) and *r* an index corresponding to a density value within the range of available masonry densities. The, decrement factors $f_{W,max}$ and $f_{W,min}$ correspond

to the maximum and minimum factors for wall formation *W*, that can be achieved by properly selecting the masonry density. An analogous notation applies for the time lag calculations.

Evidently, both PDM_W and PTM_W vary from 0 % to 100 %. By computing the above proportional metrics, for a particular wall assembly, it is possible to plot their values in a common *y*-axis of an *x*-*y* graph with the masonry densities in the *x*-axis. In this way, from the graphs of the various wall assemblies, the range of masonry density values for which acceptable inertia parameters are achieved can be easily observed.

On the other hand, in order to assess the possibility of enhancing the thermal inertia parameters of a wall formation *W*, the metrics RDM_W and RTM_W are proposed. The values of the above metrics are greater or equal to 1. A value of 1 for these metrics serves as the baseline for assessing their relative merit of the various wall assemblies. Values greater than 1 indicate that the density of the masonry material leads to a superior thermal inertia performance, compared to the base case.

The graphs of Fig. 6(a)-(f) illustrate the variations of the above proposed metrics as regards to the determined dynamic thermal characteristics.

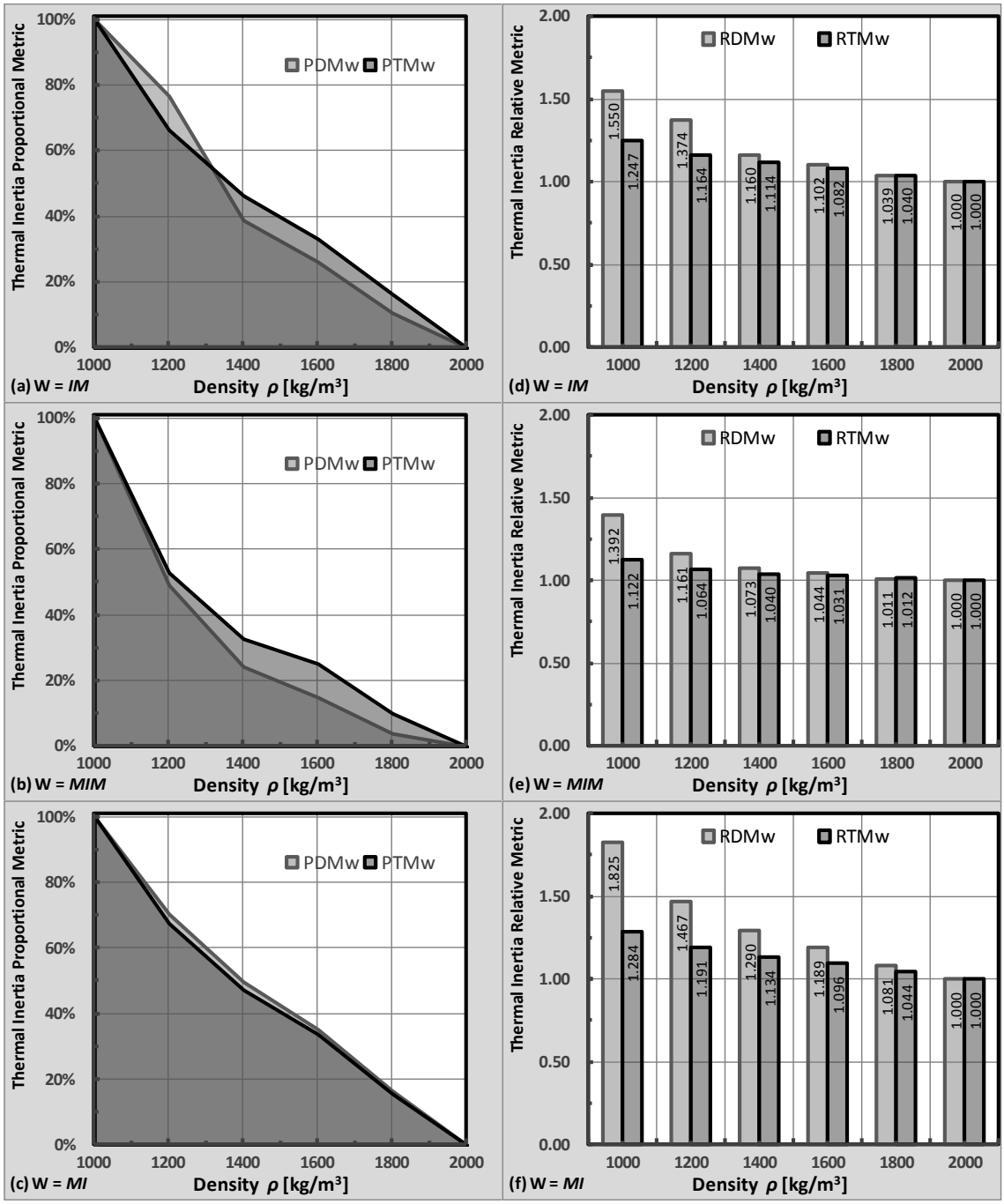

Figure 6. Thermal inertia metrics from a proportional (a)-(c) and relative (d)-(f) point of view.

For the *IM*, *MIM* and *MI* wall assemblies, the graphs in Fig. 6(a)-(c) show an almost linear decrease of *PDM* and *PTM* values, with the masonry density increase. Accordingly, the optimal and worst values of *PDM* and *PTM* are attained for ρ_M = 1000 kg/m^3 and ρ_M = 2000 kg/m^3, respectively. Moreover, the rate of declination for both metrics is virtually the same; for the *MI* wall configuration the *PDM* and *PTM* values almost coincide.

As shown in Fig. 6(d) for the *IM* wall assembly the optimal values of decrement factor and time lag are obtained for ρ_M = 1000 kg/m^3. For this case *RDM* = 1.550 and *RTM* = 1.247, suggest a possible enhancement of about 55.0% and 24.7%, for f and φ respectively. The resultant improvements for the *MIM* wall assembly, as seen in Fig. 6(e), are 39.2% and 12.2%, for f and φ respectively (*RDM* = 1.392 and *RTM* = 1.122). At last, as seen in Fig. 6(f) for the *MI* wall assembly the corresponding improvements are 82.5% and 28.4%, with regard to to f and φ respectively (*RDM* = 1.825 and *RTM* = 1.284). Evidently, it is seen that for the *MI* configuration the change of masonry density affects radically the *RDM* variation (maximum *RDM* value). Moreover, for this case the maximum *RTM* value is obtained.

6 CONCLUSIONS

In the present work the influence of the brick density and thermal conductivity variations of insulated wall assemblies on decrement factor f and time lag φ has been examined. As the masonry density varies, it has been revealed that the corresponding increase in its thermal conductivity can significantly modify its thermal inertia parameters. Computer results showed how the density and thermal conductivity variations of solid bricks as well as the relative placement of masonry and insulation affect the thermal response of the studied elements. In order to facilitate the selection of suitable values for masonry density, for each of the individual wall assemblies, so that to achieve acceptable values for the decrement factor and time lag, two relevant metrics (*PDM* / *PTM* and *RDM* / *RTM*) have been introduced. From the presented results it has been shown that the *PDM* and *PTM* metrics lead to the most adverse values for heavyweight solid bricks. Accordingly, thermal mass surpluses, as well as its corresponding low thermal resistance of multilayered wall assemblies, demonstrate a moderate thermal behavior. In another direction, the relative *RDM* and *RTM* metrics have indicated that the wall formation *MI* is more susceptible to decrement factor and time lag improvements by selecting lightweight solid bricks.

REFERENCES

[1] Asan, H. (1998), “Effects of wall’s insulation thickness and position on time lag and decrement factor”, Energy and Buildings 28(3), pp. 299-305.
[2] Asan, H. (2000), “Investigation of wall’s optimum insulation position from maximum time lag and minimum decrement factor point of view”, Energy and Buildings 32(2), pp. 197-203.
[3] Ozel, M., Pihtili K. (2007), “Optimum location and distribution of insulation layers on building walls with various orientations”, Building and Environment 42(8), pp. 3051-3059.
[4] Al-Sanea, S.A., Zedan, M.F. (2011), “Improving thermal performance of building walls by optimizing insulation layer distribution and thickness for same thermal mass”, Applied Energy 88(9), pp. 3113-3124.
[5] Al-Sanea, S.A., Zedan, M.F., Al-Hussain, S.N. (2012), “Effect of thermal mass on performance of insulated building walls and the concept of energy savings potential”, Applied Energy 89(1), pp. 430-442.
[6] Al-Sanea, S.A., Zedan, M.F., Al-Hussain, S.N. (2013), “Effect of masonry material and surface absorptivity on critical thermal mass in insulated building walls”, Applied Energy 102(2), pp. 1063-1070.
[7] Kontoleon, K.J., Eumorfopoulou, E.A. (2008), “The influence of wall orientation and exterior surface solar absorptivity on time lag and decrement factor in the Greek region”, Renewable Energy 33(7), pp. 1652-1664.
[8] Kontoleon, K.J., Theodosiou, Th.G., Tsikaloudaki, K.G. (2013), “The influence of concrete density and conductivity on walls’ thermal inertia parameters under a variety of masonry and insulation placements”, Applied Energy 112(12), pp. 325-337.
[9] Jin, X., Zhang, X., Cao, Y., Wang, G. (2012), “Thermal performance evaluation of the wall using heat flux time lag and decrement factor”, Energy and Buildings 47(4), pp. 369-374.
[10] Oldenburger, R. (1950), *Mathematical engineering analysis*, Dover Publications, New York.
[11] Threlkeld, J.L. (1970), *Thermal environmental engineering*, Prentice-Hall, Englewood Cliffs, New Jersey.
[12] Underwood, C.P., Yik, F.W.H. (2004), *Modelling methods for energy in buildings*, Blackwell Science, Oxford.
[13] Kontoleon, K.J. (2012), “Dynamic thermal circuit modelling with distribution of internal solar radiation on varying façade orientations”, Energy and Buildings 47(4), pp. 139-150.
[14] Kontoleon, K.J. (2013), “Energy Savings Assessment in Buildings with Varying Facade Orientations and Types of Glazing Systems when Exposed to Sun”, International Journal of Performability Eng. 9(1), pp. 37-52.
[15] Burberry, P. (1998), *Mitchell’s environment and services*, Longman, New York.